

Scientific Article

Geometric Reproducibility of Fiducial Markers and Efficacy of a Patient-Specific Margin Design Using Deep Inspiration Breath Hold for Stereotactic Body Radiation Therapy for Pancreatic Cancer



Sarah Han-Oh, PhD,^{a,*} Colin Hill, MD,^a Ken Kang-Hsin Wang, PhD,^a Kai Ding, PhD,^a Jean L. Wright, MD,^a Sara Alcorn, MD, MPH, PhD,^a Jeffrey Meyer, MD, MS,^a Joseph Herman, MD, MSc, MSHM,^b and Amol Narang, MD^a

^aDepartment of Radiation Oncology and Molecular Radiation Sciences, Johns Hopkins University of School of Medicine, Baltimore, Maryland; and ^bRadiation Medicine, Zucker School of Medicine at Hofstra/Northwell, Lake Success, New York

Received 20 August 2020; revised 20 December 2020; accepted 30 December 2020

Abstract

Purpose: In patients undergoing stereotactic body radiation therapy (SBRT) for pancreatic adenocarcinoma, the reproducibility of tumor positioning between deep-inspiration breath holds is unclear. We characterized this variation with fiducials at simulation and treatment and investigated whether a patient-specific breath-hold (PSBH) margin would help account for intrafraction variation at treatment.

Methods and Materials: We analyzed 20 consecutive patients with pancreatic cancer who underwent SBRT with deep-inspiration breath holds. At simulation, 3 additional breath-hold scans were acquired immediately after the contrast-enhanced planning computed tomography (CT) scan and used to quantify the mean and maximum variations in the simulation fiducial position (Sim_Var_{avg} and Sim_Var_{max}), as well as to design the internal target volume (ITV) incorporating a PSBH margin.

Results: At treatment, a mean of 5 breath-hold cone beam CT (CBCT) scans were acquired per fraction for each patient to quantify the mean and maximum variations in the treatment fiducial position (Tx_Var_{avg} and Tx_Var_{max}). Various planning target volume (PTV) margins on the gross tumor volume (GTV) versus ITV were evaluated using CBCT scans, with the goal of >95% of fiducials being covered at treatment. The Sim_Var_{avg} and Sim_Var_{max} were 0.9 ± 0.5 mm and 1.5 ± 0.8 mm in the left-right (LR) direction, 0.9 ± 0.4 mm and 1.4 ± 0.4 mm in the anteroposterior (AP) direction, and 1.5 ± 0.9 mm and 2.1 ± 1.0 mm in the superoinferior (SI) direction, respectively. The Tx_Var_{avg} and Tx_Var_{max} were 1.2 ± 0.4 mm and 2.0 ± 0.7 mm in the LR direction, 1.1 ± 0.4 mm and 1.8 ± 0.6 mm in the AP direction, and 1.9 ± 1.0 mm and 3.1 ± 1.4 mm in the SI direction, respectively. The ITV was increased by $21.0\% \pm 8.6\%$ compared with the GTV alone. The PTV margin necessary to encompass >95% of the fiducial locations was 2 mm versus 4 mm in both LR and AP and 4 mm versus 6 mm in SI for the ITV and the GTV, respectively.

Sources of support: This work had no specific funding.

Disclosures: Dr Han-Oh reports grants from Allegheny Health Network Cancer Research Fund outside the submitted work. Dr Ding reports grants from the National Institutes of Health, Elekta, and Boston Scientific outside the submitted work. Dr Meyer reports other from Boston Scientific outside the submitted work and royalties from UpToDate, Inc, and Springer. Dr Herman reports grants from OncoSil, Galera, and Augmenix and other from 1440 Foundation outside the submitted work. Dr Narang reports grants from Boston Scientific outside the submitted work.

Data Sharing Statement: All data generated and analyzed during this study are included in this published article.

Presented at the annual meeting of the American Society for Radiation Oncology, October 21 to 24, 2018, in San Antonio, Texas.

* Corresponding author: Sarah Han-Oh, PhD; E-mail: yhanoh1@jhmi.edu

<https://doi.org/10.1016/j.adro.2021.100655>

2452-1094/© 2021 The Author(s). Published by Elsevier Inc. on behalf of American Society for Radiation Oncology. This is an open access article under the CC BY-NC-ND license (<http://creativecommons.org/licenses/by-nc-nd/4.0/>).

Conclusions: The interbreath-hold variation is not insignificant, especially in the SI direction. Acquiring multiple breath-hold CT scans at simulation can help quantify the reproducibility of the interbreath hold and design a PSBH margin for treatment.

© 2021 The Author(s). Published by Elsevier Inc. on behalf of American Society for Radiation Oncology. This is an open access article under the CC BY-NC-ND license (<http://creativecommons.org/licenses/by-nc-nd/4.0/>).

Introduction

Tumors located in the abdominothoracic area, such as the lung, liver, or pancreas, are highly susceptible to clinically significant respiratory motion during radiation therapy (RT).¹⁻⁶ Many investigators have reported that tumor motion can range from 0 to 40 mm under shallow free breathing.⁷ The internal target volume (ITV) is an effective measure to account for tumor motion by encompassing the motion range as a margin. With the present use of cone beam computed tomography (CBCT) for effective patient setup, the ITV often contributes to the largest portion of the total margin, and the resultant abutment or overlap with an organ at risk (OAR) significantly compromises the ability to deliver the therapeutic radiation dose safely without inflicting deleterious toxicity. Therefore, use of tumor-motion management is imperative for safe delivery of stereotactic body radiation therapy (SBRT) to these sites, especially for pancreatic tumors, given the proximity of highly radiosensitive organs such as the duodenum and stomach.

Among various motion-mitigation techniques, including breath-hold,⁸ beam gating,⁹ and real-time tumor-motion compensation using a multileaf collimator or couch,¹⁰⁻¹² the deep-inspiration breath hold (DIBH) prevents tumor motion by asking patients to hold their breath after taking deep inspiration. The effectiveness of the DIBH largely depends on achieving consistent reproducibility of tumor positioning with each breath hold (interbreath-hold variation), especially because multiple breath holds are typically needed to complete delivery of the treatment fraction. Extensive studies in lung and liver tumors with DIBH have reported interbreath-hold variation of less than 2 mm on average, regardless of various breath-hold techniques.¹³⁻¹⁹ However, interbreath-hold reproducibility when treating pancreatic tumors with DIBH presents unique challenges because it is influenced by both the diaphragm and abutting abdominal soft tissues and has not been well characterized in a robust manner.

Three studies have reported on this subject matter, but with significant limitations. Murphy et al²⁰ reported that the 3-dimensional (3D) pancreas tumor position is reproducible within 2.5 mm, but this conclusion was based on data from only 4 patients. Nakamura et al²¹ showed that in the treatment of pancreatic tumors, the reproducibility of exhalation breath hold was 0.0 ± 1.1 mm in the left-right (LR) direction, 0.1 ± 1.2 mm in the anteroposterior (AP) direction, and 0.1 ± 1.0 mm in the

superoinferior (SI) direction, but exhalation breath-hold can be highly challenging for patients compared with inspiratory breath-hold, particularly because pancreatic cancer is a disease of the elderly. Teboh et al²² analyzed 19 patients with pancreatic cancer and reported that the intrafraction DIBH variation was contained within the 2-mm fiducial planning target volume (PTV), but this study used kV projection images at each beam angle, compared with 3D quantitative analysis based on volumetric imaging.

In the current study, we characterized the DIBH variation of pancreas tumor positioning at the time of CT simulation and RT treatment from a cohort of 20 patients. In addition, we investigated whether a patient-specific, “personalized” margin designed from the DIBH variation of tumor positioning measured at simulation can account for intrafraction variation at treatment. We also explored whether the patient-specific margin, compared with the PTV generated by a direct uniform expansion on the gross tumor volume (GTV), would achieve more optimal target and fiducial coverage during RT.

Methods and Materials

All imaging scans at simulation and treatment were acquired as part of the clinical workflow of the standard of care.

Patient selection and breath-hold coaching at simulation

We selected 20 consecutive patients who underwent SBRT using the DIBH technique for pancreatic cancer at our institution. Patients were treated with the DIBH technique if they could inhale and hold greater than 1 L of air for more than 20 seconds consistently, per our institution’s protocol. In the calendar year during which these patients were treated, 81.3% of the patients were treated with the DIBH technique, suggesting that this analysis may be applicable to the vast majority of patients eligible for pancreatic SBRT. Patients were asked to fast 3 to 5 hours before both the simulation and the treatment to provide reproducible gastric organ positioning. Patients were immobilized with a wing-board (CIVCO Medical Solutions, Coralville, IA) and either an alpha cradle (Smithers Medical Products Inc, North Canton, OH) or a Vac-Lok (CIVCO Medical Solutions). Active Breathing Coordinator 3.0 (ABC, Elekta, Stockholm, Sweden) was

used to assist patients' breath hold without visual feedback of the breathing traces. We coached the patients to take air in while minimizing their physical body movement, such as arching of the spine. After the successful breathing coaching, a treatment planning CT was acquired after intravenous contrast injection (Omnipaque 100 mL, GE Healthcare, Chicago, IL), usually at 70 seconds after injection, to highlight the portal venous phase. Subsequently, 3 additional breath-hold CT sets were acquired. No specific timing was mandated for these 3 CT sets. Instead, the CT scans were acquired when the patient had recovered from the prior breath hold, to mimic the treatment process. Each CT set was acquired in the range of 15 to less than 20 seconds in 1 breath hold with the CT scan parameters of 120 kVp and 2-mm slice thickness.

Treatment planning and fiducial marker contouring

Each patient had 2 or 3 fiducial markers implanted endoscopically into the tumor; these were used as the tumor position surrogates. All fiducial markers were contoured on the planning CT in addition to the tumor and OAR structures. The rigid image registration was performed in Velocity (Varian Medical Systems, Inc, Palo Alto, CA) to propagate the fiducial contours from the planning CT to the additional 3 CT sets. Each fiducial contour was fine-tuned to confirm to the corresponding fiducial location. The centroid of each fiducial marker was calculated from the contours. To accommodate 2 intra-fraction breath-hold CBCT scans, a single 360-degree sweep volumetric modulated arc therapy (VMAT) divided into 3 partial arcs was planned with a prescription of 660 cGy x 5 fractions in Pinnacle 9.2 (Philips Healthcare, Amsterdam, Netherlands).

Patient setup and fiducial contouring on breath-hold CBCT at treatment

Before treatment started, multiple breath-hold CBCT scans were acquired using Elekta XVI 5.2 to set up the patient to the treatment position with a rescanning tolerance of 1.5 mm in any anatomic direction. During treatment, 2 breath-hold CBCT scans were acquired between the partial VMAT arcs. An additional CBCT scan was acquired if the table shift exceeded the rescanning tolerance. Each CBCT scan was acquired in 1 to 2 breath holds with a fast partial arc (200-degree sweep) and a segmental VolumeView license (Elekta). The CBCT scans were aligned to the planning CT with a 2-step rigid image registration process and aligned to the spine, followed by the fiducial markers. The propagated fiducial contours on the CBCT scan were used to calculate the centroids of the fiducial markers.

Quantification of interbreath-hold variation

The interbreath-hold variation at simulation and treatment as calculated for an individual patient is described below.

Variation at CT simulation

Each simulation CT acquired with 1 breath hold had multiple fiducial markers. The centroids of the individual fiducials from the planning CT were used as the reference and were compared with those from the subsequent CT sets to quantify the interbreath-hold variation. The variation at CT simulation was measured within the same session and was categorized as intrafractional variation. For the CT set i , the positional variation of the fiducial j , $\Delta x_{i,j}^{SIM}$, was calculated by subtracting the centroid in the reference CT, $x_{0,j}^{SIM}$, from that of the same fiducial in the image i , $x_{i,j}^{SIM}$, using Eq 1. The reference CT was labeled as $i = 0$. The average difference of all fiducials calculated by Eq 2 was defined as the interbreath-hold variation for the CT set i .

$$\Delta x_{i,j}^{SIM} = \left| x_{i,j}^{SIM} - x_{0,j}^{SIM} \right| \quad (1)$$

$$\overline{\Delta x}_i^{SIM} = \frac{\sum_{j=1}^{N_{fid}} \Delta x_{i,j}^{SIM}}{N_{fid}} \quad (2)$$

where $\overline{\Delta x}_i^{SIM}$ is the average variation of all fiducial markers in the given CT set i and N_{fid} is the number of the implanted fiducial markers.

To represent interbreath-hold variation at simulation for each patient, the average and maximum variations from all 3 CT sets, SIM_Var_{avg} and SIM_Var_{max} , were calculated using Eqs 3 and 4:

$$SIM_Var_{avg} = \frac{\sum_{i=1}^{N_I} \overline{\Delta x}_i^{SIM}}{N_I} \quad (3)$$

$$SIM_Var_{max} = \text{Max} \left(\overline{\Delta x}_i^{SIM} \right) \quad (4)$$

where N_I is the number of the CT sets, which was 3 for each patient.

The calculations defined in Eqs 1 to 4 were performed for each anatomic direction: LR, AP, and SI.

Variation at treatment

We acquired, on average, 5.0 ± 0.7 breath-hold CBCT scans per fraction for each patient, totaling 25.0 ± 3.3 images for 5 fractions, as summarized in Table 1. The interbreath-hold variation at treatment was calculated using the same method as described in the previous section, using the first CBCT scan for that fraction as the

Table 1 Patients' demographics and breath-hold characteristics

Patient	Age, y	Sex	No. of fiducial markers	Breath hold parameters		Breath hold simulation CT sets, No.	No. of breath hold CBCT scans				
				Threshold, L	Duration, s		FX 1	FX 2	FX 3	FX 4	FX 5
1	71	M	3	4.0	60	4	5	4	6	4	7
2	52	M	3	2.0	40	4	3	8	5	5	4
3	66	F	3	1.8	30	4	6	7	5	8	3
4	72	M	3	2.6	40	4	4	4	5	4	4
5	56	M	3	1.7	30	4	4	4	5	5	4
6	53	F	3	1.0	25	4	6	6	6	5	5
7	75	M	3	2.1	35	4	6	6	7	4	6
8	61	M	2	1.8	35	4	5	4	4	4	5
9	63	F	3	1.2	25	4	4	4	4	5	6
10	69	M	3	1.9	30	4	5	4	4	4	4
11	78	M	3	1.9	35	4	7	4	4	4	6
12	58	F	3	1.0	18	4	9	5	4	6	4
13	63	M	3	1.8	30	4	5	4	4	6	4
14	68	F	3	1.0	30	4	4	4	4	4	4
15	65	M	3	2.0	30	4	6	5	5	5	5
16	69	F	3	1.0	25	4	4	5	5	8	5
17	72	F	3	1.8	30	4	7	5	5	4	6
18	79	F	3	1.3	30	4	6	4	4	5	5
19	69	F	3	1.5	30	4	5	4	5	4	4
20	53	F	3	1.3	30	4	7	5	8	8	4

Abbreviations: CBCT = cone beam computed tomography; CT = computed tomography; FX = fraction.

reference and using similar metrics to characterize fiducial position variation, as shown in Eqs 5 to 7:

$$\Delta x_{ij}^k = |x_{ij}^k - x_{0j}^k| \quad (5)$$

$$\overline{\Delta x}_i^k = \frac{\sum_{j=1}^{N_{fid}} \Delta x_{ij}^k}{N_{fid}} \quad (6)$$

$$\overline{\Delta x}_{max}^k = \text{Max}(\overline{\Delta x}_i^k) \quad (7)$$

where x_{0j}^k and x_{ij}^k are the centroids of the fiducial j in the first CBCT scan ($i = 0$) and the CBCT set i acquired at treatment fraction k , respectively; $\overline{\Delta x}_i^k$ is the average variation of all fiducial markers in the CBCT set i at treatment fraction k ; N_{fid} is the number of implanted fiducial markers; and Δx_{max}^k is the maximum variation for fraction k . The shift to the fiducial markers calculated in the first CBCT scan, defined as interfraction variation, was not included in the analysis.

To quantify the variation at the course of treatment, 2 metrics were defined using Eqs 8 and 9: the average variation, TX_Var_{avg} , from all CBCT sets acquired from 5 fractions and the average maximum, TX_Var_{max} , of all 5 maximum values from 5 fractions.

$$TX_Var_{avg} = \frac{\sum_{k=1}^{N_{FX}} \sum_{i=1}^{N_i^k} \overline{\Delta x}_i^k}{N_{FX} N_i^k} \quad (8)$$

$$TX_Var_{max} = \frac{\sum_{k=1}^{N_{FX}} \overline{\Delta x}_{max}^k}{N_{FX}} \quad (9)$$

where N_i^k is the number of the CBCT sets acquired at fraction k and N_{FX} is the number of fractions, which was 5. The variations were calculated for each anatomic direction: LR, AP, and SI.

Usefulness of a patient-specific breath-hold margin design

The ITV incorporating a patient-specific interbreath-hold variation was designed by combining all 4 sets of tumor contours from the 4 simulation CT sets and comparing them with the GTV contoured from the planning CT only. A ratio of ITV to GTV was calculated to indicate a volume increase with a patient-specific breath-hold margin. The $ITV_{fiducial j}$ for the fiducial marker j was also generated by combining all 4 fiducial contours from the repeated CT sets. The fiducial contour in the planning CT only was defined as $GTV_{fiducial j}$. We expanded the fiducial GTV and ITV with an isotropic PTV margin. For each fiducial, 6 PTVs were generated, with expansions ranging from 1 mm to 6 mm in 1-mm increments. From

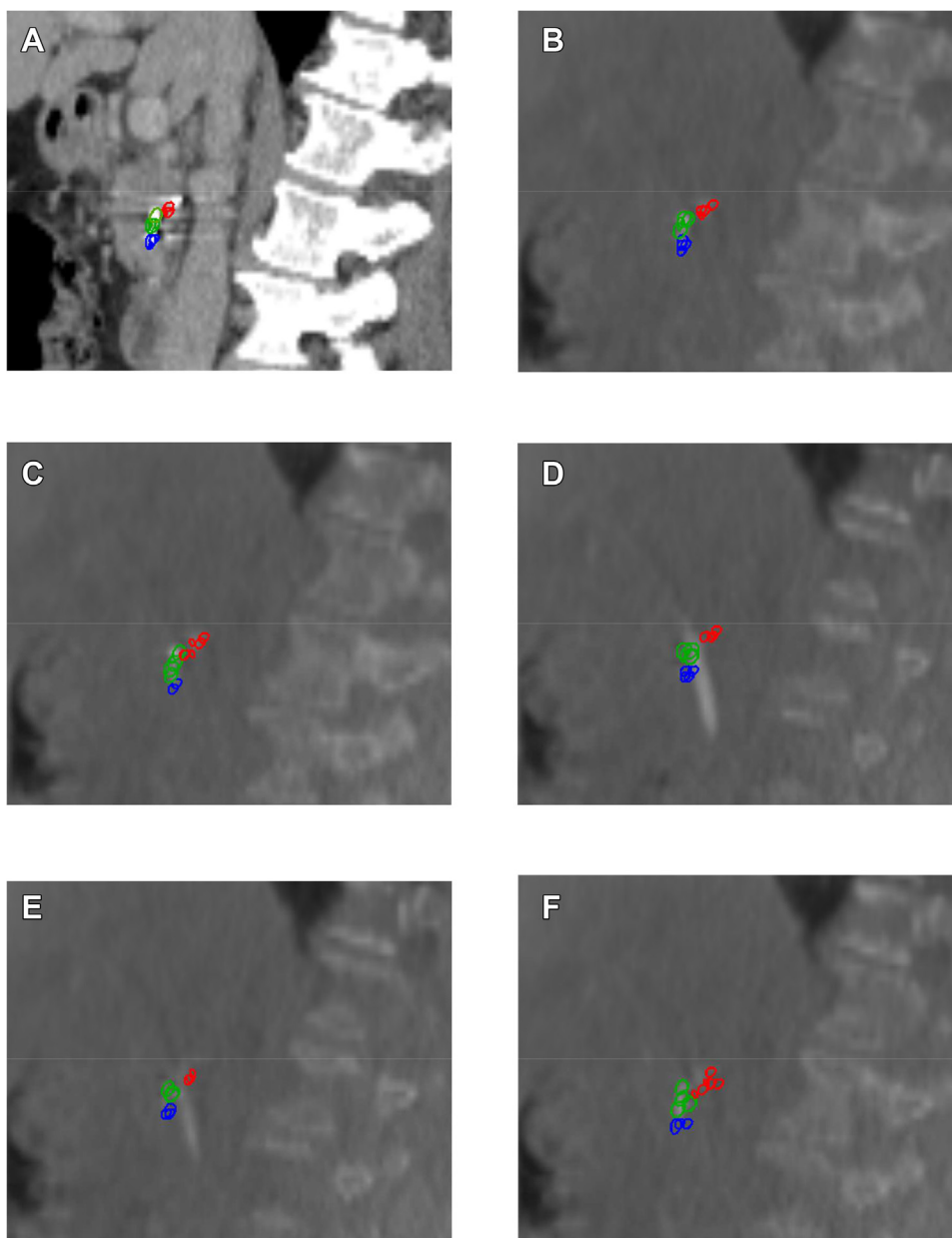


Figure 1 Sagittal view of interbreath-hold variations of patient 17 at simulation and 5 treatment fractions: A, simulation; B, fraction 1; C, fraction 2; D, fraction 3; E, fraction 4; and F, fraction 5. The red, green, and blue colors are fiducial locations overlaid from all breath holds for each fraction. The interbreath-hold variation is clearly shown with a varying amount for each fraction.

the breath-hold CBCT sets, we quantified the percentage of the fiducial locations within each PTV to evaluate the usefulness of a patient-specific breath-hold margin design to account for the variation at treatment.

Statistical analysis

A Student *t* test was performed to assess statistical significance in the differences; significance was set at $P < .05$.

Results

Interbreath hold variation at simulation and treatment

[Table 1](#) summarizes patients' demographics and breath-hold parameters. The median age of the selected patients was 67 years, ranging from 52 to 79 years, with an equal male-to-female ratio. The mean air-volume threshold and duration of breath hold were 1.7 ± 0.7 L

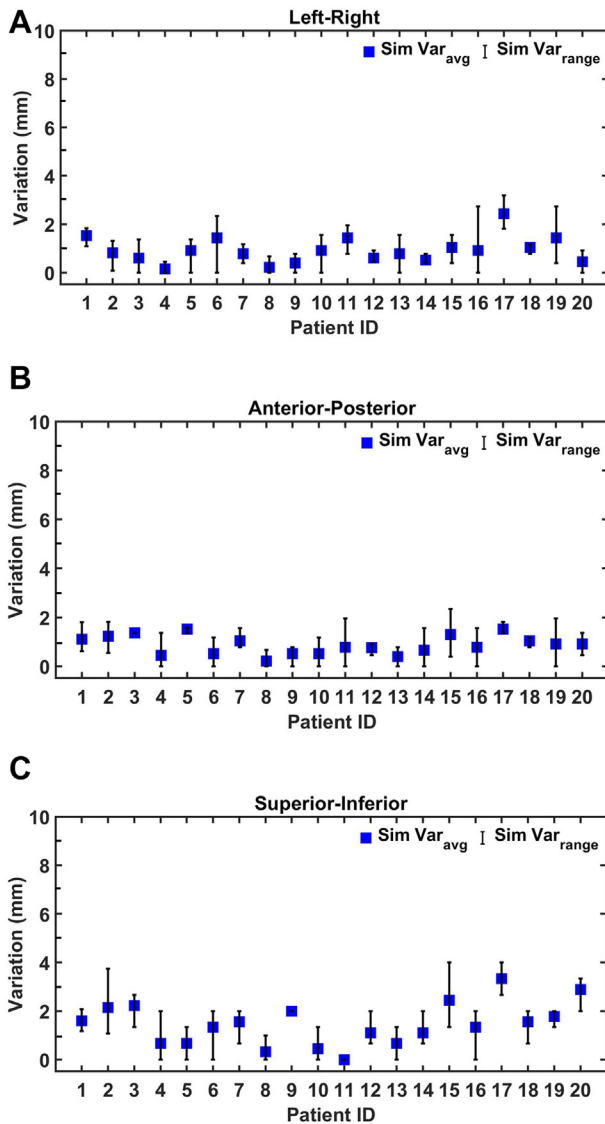


Figure 2 Interbreath-hold variation from 4 simulation computed tomography sets for individual patients. The square represents average variation; the error bar shows the range of the data (minimum to maximum).

(range, 1.0–4.0 L) and 31.9 ± 8.3 seconds (range, 18.0–60.0 seconds).

Figure 1 shows the extreme interbreath-hold variations of patient 17 at CT simulation and treatment. The patient showed Sim_Var_{avg} and Sim_Var_{max} values of 2.4 ± 0.7 mm and 3.2 mm in LR, 1.5 ± 0.3 mm and 1.8 mm in AP, and 3.3 ± 0.7 mm and 4.0 mm in SI. The Tx_Var_{avg} and Tx_Var_{max} values, averaged over all 5 fractions, were 1.4 ± 0.4 mm and 2.5 ± 1.8 mm in the LR direction, 1.6 ± 0.4 mm and 2.8 ± 0.9 mm in the AP direction, and 2.4 ± 1.7 mm and 3.6 ± 2.7 mm in the SI direction.

Figures 2 and 3 show interbreath-hold variations of the 20 individual patients at simulation and treatment. The variation in the SI direction was significantly larger than in the LR and AP directions at both CT simulation and

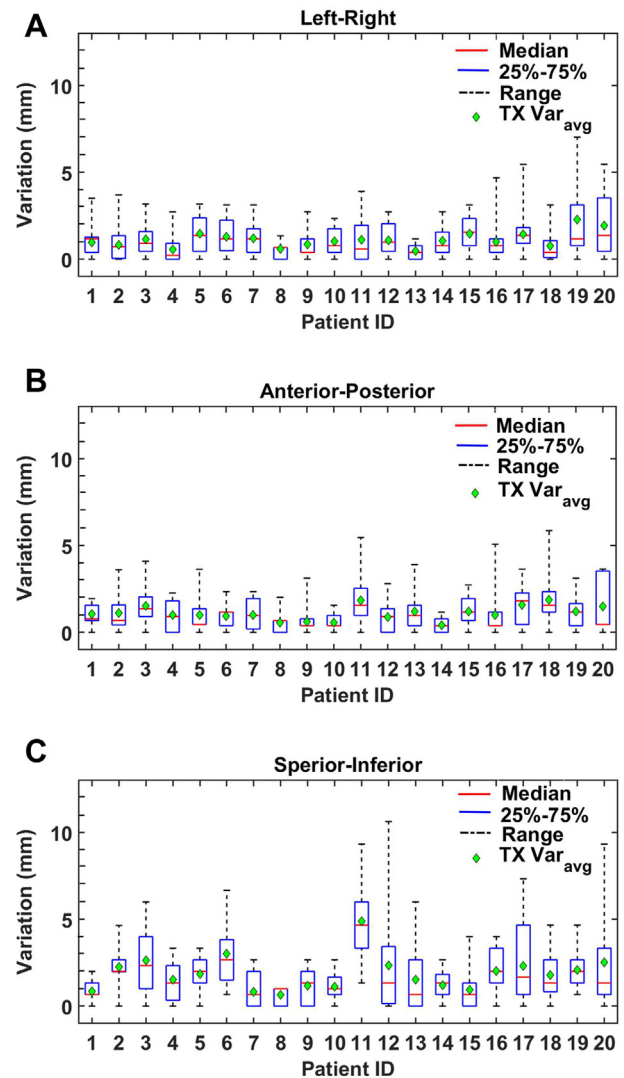


Figure 3 Interbreath-hold variation measured from multiple breath-hold cone beam computed tomography sets at treatment. The diamond represents the average variation; the red line represents the median value; the box represents the range from the 25th to 75th quartile; and the whisker represents the range (minimum to maximum). Patients 1 and 8 showed reproducible interbreath-hold variation at both computed tomography simulation and treatment, whereas patient 11 showed increased variation at treatment compared with at computed tomography simulation.

treatment ($P < .05$). There was no significant difference between the LR and AP directions ($P > .05$). Some patients, such as patients 1 and 8, showed reproducible variations at both simulation and treatment, whereas patient 11 showed a larger variation at treatment than at CT simulation. The reproducibility of breath hold between CT simulation and treatment was also highly patient-dependent.

Table 2 summarizes the variations at CT simulation and treatment, averaged over all 20 patients. The

Table 2 The mean (± 1 standard deviation) of interbreath-hold variations averaged over all 20 patients at computed tomography simulation and treatment

	<i>Sim_Var_{avg}</i> (mm)	<i>Tx_Var_{avg}</i> (mm)	<i>P</i> value
LR	0.9 \pm 0.5	1.2 \pm 0.4	.069
AP	0.9 \pm 0.4	1.1 \pm 0.4	.057
SI	1.5 \pm 0.9	1.9 \pm 1.0	.099
	<i>Sim_Var_{max}</i> (mm)	<i>Tx_Var_{max}</i> (mm)	<i>P</i> value
LR	1.5 \pm 0.8	2.0 \pm 0.7	.057
AP	1.4 \pm 0.4	1.8 \pm 0.6	.028
SI	2.1 \pm 1.0	3.1 \pm 1.4	.016

Abbreviations: AP = anteroposterior; LR = left-right; SI = superoinferior; *Sim_Var_{avg}* = average variation in the simulation fiducial position; *Tx_Var_{avg}* = average variation in the treatment fiducial position.

Tx_Var_{avg} values were not significantly different than the *Sim_Var_{avg}* values, but the *Tx_Var_{max}* values increased significantly in the AP and SI directions ($P < .05$). The *Sim_Var_{max}* and *Tx_Var_{max}* values showed a moderate positive linear relationship with a correlation coefficient of 0.343 ($P = .007$). The *Tx_Var_{max}* value was within the 95% prediction interval of *Sim_Var_{max}* which indicated that the *Sim_Var_{max}* value was a predictive metric for treatment variation. The *Tx_Var_{max}* value was not significantly correlated to the breath-hold air-volume threshold in the patient cohort ($P > .05$).

Usefulness of a patient-specific breath-hold margin design

The ITV was increased by 21.0% \pm 8.6% compared with the GTV. The mean percentage of fiducial location within the various PTV margins is shown in Table 3. The 2-mm uniform margin added to the GTV covers 83.2% \pm 12.5% in the LR direction, 84.5% \pm 11.3% in the AP direction, and 69.2% \pm 24.1% in the SI direction. To cover 95% of the fiducial locations at treatment, an asymmetrical margin design measuring 4 mm in both the

LR and AP directions and 6 mm in the SI direction was necessary for the GTV. With the patient-specific breath-hold margin design, the 2-mm margin was enough for both the AP and LR directions, but 4 mm was necessary in the SI direction. When applying the suggested asymmetrical margin to each approach, the PTV was increased by 67.5% \pm 12.5% for the GTV and 60.2% \pm 16.7% for the ITV ($P < .05$) compared with the 2-mm uniform PTV margin expansion from the GTV. This shows the usefulness of the patient-specific margin design. In comparison, the uniform margin expansion, 6 mm on the GTV and 4 mm on the ITV, increased the PTV by 92.4% \pm 19.4% and 81.5% \pm 22.7%, respectively.

Discussion

Deep-inspiration breath hold is a widely used motion management technique in clinic. Understanding of the interbreath-hold reproducibility in tumor positioning is important to achieve an intended target coverage and normal tissue sparing during radiation treatment, especially for pancreas tumors that are closely surrounded by OARs, including the small bowel and stomach. The positional reproducibility of pancreas tumors between breath holds has not been well elucidated compared with other disease sites, such as the lungs or liver. In this study, we calculated that the pancreas tumor position is reproducible to less than 3 mm, on average, in all 3 anatomic directions at both simulation and treatment. However, the variation is highly patient-dependent, and the range of the variation is large among patients. The mean variation is slightly larger than the reported values for lung or liver tumors but comparable with results reported for the pancreas.²⁰ Regardless of the disease site, the variation is the largest in the SI direction, which suggests the necessity of asymmetrical margin design. The margin may be able to be reduced when real-time intrafractional imaging, such as kV fluoroscopy, ultrasound, electromagnetic tracking, or a magnetic resonance linear accelerator, is used for tumor-position verification for each breath hold.

Table 3 Percentage of the fiducial location within the PTV at treatment, averaged over all 20 patients

PTV margin (mm)	LR		AP		SI	
	Single BH GTV	Multiple BH ITV	Single BH GTV	Multiple BH ITV	Single BH GTV	Multiple BH ITV
1	56.7 \pm 14.4	90.8 \pm 10.5	55.3 \pm 20.0	90.2 \pm 10.9	38.9 \pm 24.2	82.0 \pm 23.7
2	83.2 \pm 12.5	97.1 \pm 7.0*	84.5 \pm 11.3	95.6 \pm 7.0*	69.2 \pm 24.1	89.0 \pm 21.5
3	92.6 \pm 10.7	98.7 \pm 4.1	93.1 \pm 18.6	99.0 \pm 2.1	81.8 \pm 19.4	92.4 \pm 17.2
4	98.2 \pm 4.2*	99.3 \pm 2.1	98.8 \pm 2.7*	99.7 \pm 1.2	90.8 \pm 14.9	95.4 \pm 13.5*
5	98.8 \pm 3.1	100.0 \pm 0.0	99.3 \pm 1.8	100.0 \pm 0.0	93.7 \pm 11.4	97.1 \pm 10.1
6	99.4 \pm 2.6	100.0 \pm 0.0	100.0 \pm 0.0	100.0 \pm 0.0	96.9 \pm 6.1*	98.6 \pm 4.8

Abbreviations: AP = anteroposterior; BH = breath hold; GTV = gross tumor volume; ITV = internal target volume; LR = left-right; PTV = planning target volume; SI = superoinferior.

* The smallest margins providing greater than 95% coverage for the approach.

The study's results show that the uniform 2-mm expansion directly from the GTV contoured from a single CT set, which was our institution's approach, is not enough to provide tumor coverage greater than 95%. We suggest an asymmetrical PTV margin of 4 mm in both the LR and AP directions and 6 mm in the SI direction when a single CT set is used to design the PTV. The benefit of using multiple breath-hold CT scans is to quantify patient-specific breath-hold uncertainty and incorporate it into a PTV margin design. Additionally, the multiple CT scans can be used to screen out patients ineligible for breath-hold treatment by quantifying the maximum variation as a good indicator of a possible large variation at treatment. The patient-specific margin would be desirable over the population-averaged margin, especially for a pancreatic tumor closely abutting OARs, because the population-averaged margin might be too large for certain patients with reproducible breath hold. Because interbreath-hold variation tends to increase at treatment, the union of multiple GTVs contoured from the multiple CT sets would provide better tumor/fiducial coverage, compared with using an average variation. The suggested PTV margin for the breath-hold ITV approach is 2 mm in both the LR and AP directions and 4 mm in the SI direction.

The acquisition of multiple simulation CT sets increases the imaging dose. However, when patient-specific interbreath-hold uncertainty is not considered at the treatment planning stage, multiple CBCT scans are likely acquired to set up a patient. As a result, the cumulative imaging dose for an entire treatment course can be more than a few additional simulation CT sets. For example, 2 additional CBCT scans acquired at each fraction can be summed up to 10 CBCT scans for 5-fraction treatment, which can result in a higher imaging dose compared with 3 additional simulation CT sets. Thus, we argue that the multiple simulation CT sets are beneficial to account for interbreath-hold variation with a modest increase in imaging dose.

The interbreath-hold variation in this study did not show a strong correlation with the breath-hold threshold of the patient cohort we analyzed. In addition, the variation did not show a significant increase as the number of acquired CBCT scans was increased during treatment ($P > .05$). We hypothesize that a change in breathing technique between diaphragmatic and chest breathing can be a major contributing factor to tumor-position variation, even though the inspiration air volume is reproducibly cut off by a spirometer. The same hypothesis was mentioned by Mittauer et al.²³

In this study, the patients received no audiovisual feedback of their breathing traces at either simulation or treatment. The maximum variation of the tumor position in both the AP and SI directions was increased at treatment compared with simulation. One possible reason is that the planning CT was acquired right after breathing coaching, whereas neither extra breathing training nor a

practice session was provided for treatment. Provision of audiovisual feedback of the breathing traces to patients might help reduce the variation during treatment.

A limitation of this study was that the interbreath-hold variation was quantified using breath-hold CBCT scans acquired before and between turning on the treatment beam. The variation during treatment-beam delivery can be different from that acquired at the pretreatment imaging for patient setup. Intrafractional imaging acquired simultaneously during the treatment beam delivery—for example, simultaneous CBCT scan acquisition during VMAT delivery or biplane kV fluoroscopy—is a future step to quantify interbreath-hold variation and an adequate breath-hold margin design.

The current study focused on the geometric variation of tumor positioning between breath holds. The OARs can also show variations in their positioning, owing to both breathing uncertainty and peristalsis. Topics for future study include quantification of this motion; a dosimetric consequence of the interbreath-hold variations in tumor and OAR locations, especially for SBRT scans requiring a steep dose gradient outside the PTV to reduce a high dose to the duodenum and stomach; and proton treatment, which is sensitive to anatomic variations.

Conclusion

We quantified interbreath-hold variation in pancreas-tumor positioning at simulation and treatment. The variation was patient-specific and asymmetrical in the anatomic directions, and it increased at treatment. The variation in the SI direction was larger than in the other anatomic directions. An asymmetrical PTV margin greater than 4 mm was necessary to better account for interbreath-hold variability and resulted in better disease/fiducial coverage during treatment when a single CT set was used. The multiple CT sets acquired at simulation would be beneficial in designing a patient-specific breath-hold margin, especially for situations in which intrafraction imaging is not readily available. Additionally, some patients who show reduced interbreath-hold variation may benefit from a smaller overall expansion, whereas the population-averaged margin may be unnecessarily generous.

References

1. Bryan PJ, Custar S, Haaga JR, Balsara V. Respiratory movement of the pancreas: An ultrasonic study. *J Ultrasound Med*. 1984;3:317-320.
2. Suramo I, Päivänsalo M, Myllylä V. Cranio-caudal movements of the liver, pancreas and kidneys in respiration. *Acta Radiol Diagn (Stockh)*. 1984;25:129-131.
3. Barnes EA, Murray BR, Robinson DM, Underwood LJ, Hanson J, Roa WH. Dosimetric evaluation of lung tumor immobilization using

- breath hold at deep inspiration. *Int J Radiat Oncol*. 2001;50:1091-1098.
4. Seppenwoolde Y, Shirato H, Kitamura K, et al. Precise and real-time measurement of 3D tumor motion in lung due to breathing and heartbeat, measured during radiotherapy. *Int J Radiat Oncol Biol Phys*. 2002;53:822-834.
 5. Erridge SC, Seppenwoolde Y, Muller SH, et al. Portal imaging to assess set-up errors, tumor motion and tumor shrinkage during conformal radiotherapy of non-small cell lung cancer. *Radiation Oncol*. 2003;66:75-85.
 6. Grills IS, Yan D, Martinez AA, Vicini FA, Wong JW, Kestin LL. Potential for reduced toxicity and dose escalation in the treatment of inoperable non-small-cell lung cancer: A comparison of intensity-modulated radiation therapy (IMRT), 3D conformal radiation, and elective nodal irradiation. *Int J Radiat Oncol Biol Phys*. 2003;57:875-890.
 7. Keall PJ, Mageras GS, Balter JM, et al. The management of respiratory motion in radiation oncology report of AAPM Task Group 76. *Med Phys*. 2006;33:3874-3900.
 8. Hanley J, Debois MM, Mah D, et al. Deep inspiration breath-hold technique for lung tumors: The potential value of target immobilization and reduced lung density in dose escalation. *Int J Radiat Oncol Biol Phys*. 1999;45:603-611.
 9. Ohara K, Okumura T, Akisada M, et al. Irradiation synchronized with respiration gate. *Int J Radiat Oncol Biol Phys*. 1989;17:853-857.
 10. Keall PJ, Nguyen DT, O'Brien R, et al. The first clinical implementation of real-time image-guided adaptive radiotherapy using a standard linear accelerator. *Radiation Oncol*. 2018;127:6-11.
 11. D'Souza WD, Naqvi SA, Yu CX. Real-time intra-fraction-motion tracking using the treatment couch: a feasibility study. *Phys Med Biol*. 2005;50:4021-4033.
 12. Yi BY, Han-Oh S, Lerma F, Berman BL, Yu C. Real-time tumor tracking with preprogrammed dynamic multileaf-collimator motion and adaptive dose-rate regulation. *Med Phys*. 2008;35:3955-3962.
 13. Peng Y, Vedam S, Chang JY, et al. Implementation of feedback-guided voluntary breath-hold gating for cone beam CT-based stereotactic body radiotherapy. *Int J Radiat Oncol Biol Phys*. 2011;80:909-917.
 14. Josipovic M, Persson GF, Dueck J. Geometric uncertainties in voluntary deep inspiration breath hold radiotherapy for locally advanced lung cancer. *Radiation Oncol*. 2016;118:510-514.
 15. Cheung PCF, Sixel KC, Tirona R, Ung RC. Reproducibility of lung tumor position and reduction of lung mass within the planning target volume using active breathing control (ABC). *Int J Radiat Oncol Biol Phys*. 2003;23:1437-1442.
 16. Kimura T, Hirokawa Y, Murakami Y, et al. Reproducibility of organ position using voluntary breath-hold method with spirometer for extracranial stereotactic radiotherapy. *Int J Radiat Oncol Biol Phys*. 2004;60:1307-1313.
 17. Kimura T, Murakami Y, Kenjo M, et al. Interbreath-hold reproducibility of lung tumour position and reduction of the internal target volume using a voluntary breath-hold method with spirometer during stereotactic radiotherapy for lung tumours. *Br J Radiol*. 2007;80:355-361.
 18. Muralidhar KR, Murthy PN, Mahadev DS, Subramanyam K, Sudarshan G, Raju AK. Magnitude of shift of tumor position as a function of moderated deep inspiration breath-hold: An analysis of pooled data of lung patients with active breath control in image-guided radiotherapy. *J Med Phys*. 2008;33:147-153.
 19. Eccles C, Brock KK, Bissonnette JP, Hawkins M, Dawson LA. Reproducibility of liver position using active breathing coordinator for liver cancer radiotherapy. *Int J Radiat Oncol Biol Phys*. 2006;64:751-759.
 20. Murphy MJ, Martin D, Whyte R, Hai J, Ozhasoglu C, Le QT. The effectiveness of breath-holding to stabilize lung and pancreas tumors during radiosurgery. *Int J Radiat Oncol Biol Phys*. 2002;53:475-482.
 21. Nakamura M, Shibuya K, Shiinoki T, et al. Positional reproducibility of pancreatic tumors under end-exhalation breath-hold conditions using a visual feedback technique. *Int J Radiat Oncol Biol Phys*. 2011;79:1565-1571.
 22. Teboh RF, Srinivasan S, Ng SP, Aliru ML, Herman JM. Setup management for stereotactic body radiation therapy of patients with pancreatic cancer treated via the breath-hold technique. *Pract Radiat Oncol*. 2020;10:e280-e289.
 23. Mittauer KE, Deraniyagala R, Li JG, et al. Monitoring ABC-assisted deep inspiration breath hold for left-sided breast radiotherapy with an optical tracking system. *Med Phys*. 2015;42:134-143.